scientific reports

Check for updates

OPEN

Liver-derived cell lines from cavefish *Astyanax mexicanus* as an in vitro model for studying metabolic adaptation

Jaya Krishnan[1]✉, Yan Wang[1], Olga Kenzior[1], Huzaifa Hassan[1], Luke Olsen[1,2], Dai Tsuchiya[1], Alexander Kenzior[1], Robert Peuß[1,3], Shaolei Xiong[1,4], Yongfu Wang[1], Chongbei Zhao[1] & Nicolas Rohner[1,2]✉

Cell lines have become an integral resource and tool for conducting biological experiments ever since the Hela cell line was first developed (Scherer et al. in J Exp Med 97:695–710, 1953). They not only allow detailed investigation of molecular pathways but are faster and more cost-effective than most in vivo approaches. The last decade saw many emerging model systems strengthening basic science research. However, lack of genetic and molecular tools in these newer systems pose many obstacles. *Astyanax mexicanus* is proving to be an interesting new model system for understanding metabolic adaptation. To further enhance the utility of this system, we developed liver-derived cell lines from both surface-dwelling and cave-dwelling morphotypes. In this study, we provide detailed methodology of the derivation process along with comprehensive biochemical and molecular characterization of the cell lines, which reflect key metabolic traits of cavefish adaptation. We anticipate these cell lines to become a useful resource for the *Astyanax* community as well as researchers investigating fish biology, comparative physiology, and metabolism.

Astyanax mexicanus has emerged as a powerful system to understand the genetic and physiological basis of metabolic adaptation to nutrient deprived habitats[2–10]. The species comes in two morphotypes—the surface fish that live in lush, nutrient-rich rivers and the blind cavefish that dwell in dark and nutrient-poor caves in the Sierra de El Abra of northeast Mexico. The cavefish survive the nutrient-deprived conditions by remodeling their metabolism, accumulating fat stores, and becoming hyperglycemic when food is available[8,10]. The liver plays an essential role in this process as a key organ for integration of fat and glucose metabolism and thereby, metabolic adaptation. Previous studies from our lab have shown that cavefish have fatty livers and show differential regulation of many key metabolic genes combined with massive differences in chromatin architecture that correlate with gene expression changes[4,8]. Cell cultures, from various tissues and embryos, from several organisms are now available including multiple cell lines from human, mouse, zebrafish, rainbow trout, Somalian cavefish etc.[11–15]. These in vitro systems have proven invaluable for many biochemical, toxicology and cell biology experiments. With the availability of gene editing technologies and high-throughput reporter assays enabling rapid and detailed characterization of genes and regulatory elements, there is a need to develop cell lines for *Astyanax mexicanus*. To this end, we have generated cell lines from surface fish livers (SFL) and Pachón cavefish livers (CFL).

The SFL and CFL are adherent cells, have epithelial cell-like morphology and can be easily grown and maintained in cell culture facility. In this study, we have characterized the cell lines for multiple parameters such as liver enzyme activity, karyotyping, and transcriptome. The cells simulate several features that are seen in the fish liver physiology and thus are set to become a useful in vitro model to study the genetic and molecular underpinnings of metabolic adaptation of *Astyanax mexicanus*.

Methods

The study was carried out in compliance with the ARRIVE guidelines (https://arriveguidelines.org)[16].

[1]Stowers Institute for Medical Research, Kansas City, MO, USA. [2]Department of Molecular and Integrative Physiology, University of Kansas Medical Center, Kansas City, KS, USA. [3]Present address: Institute for Evolution and Biodiversity, University of Münster, Münster, Germany. [4]Present address: Department of Genetics, Perelman School of Medicine, Philadelphia, PA, USA. ✉email: jak@stowers.org; nro@stowers.org

Astyanax husbandry and euthanasia. *Astyanax* are housed in polycarbonate or glass fish tanks on racks (Pentair, Apopka, FL) with a 14:10 h light:dark photoperiod. Each rack uses an independent recirculating aquaculture system with mechanical, chemical, and biologic filtration, and UV disinfection. Water quality parameters are maintained within safe limits (upper limit of total ammonia nitrogen range 1 mg/L; upper limit of nitrite range 0.5 mg/L; upper limit of nitrate range 60 mg/L; temperature set-point of 22 °C; pH 7.65, specific conductance 800 µS/cm; dissolved oxygen > 90%. Water changes range from 20 to 30% daily (supplemented with Instant Ocean Sea Salt [Blacksburg, VA]). Adult fish are fed three times a day during breeding weeks and once per day during non-breeding weeks on a diet of Mysis shrimp (Hikari Sales USA, Inc., Hayward, CA) and Gemma 800 (Skretting USA, Tooele, UT). *Astyanax* husbandry and euthanasia [via Tricaine Methanesulfonate (MS222)] was approved by the Institutional Animal Care and Use Committee (IACUC) of the Stowers Institute for Medical Research on protocols 2021-122 and 2021-129. All methods were performed in accordance with the approved guidelines and regulations. The aquatic cavefish program meets all federal regulations and has been fully accredited by the Association for Assessment and Accreditation of Laboratory Animal Care (AAALAC) International since 2005.

Media composition. The complete media (ZFL-c) composition was adopted from the media used for a zebrafish liver cell line with minor changes[17], consisting of 45% Leibovitz's L-15, 30% Dulbecco's modified Eagle's and 15% Ham's F12, 15 mM Hepes–NaOH, 0.01 mg/ml bovine insulin, 50 ng/ml mouse epidermal growth factor, 5% heat-inactivated fetal bovine serum, 0.5% Trout serum and 1% embryo extract. The embryo extract was used for the initial ~ 10–15 passages until the cell lines stabilized. Extracts from 3 dpf (days post fertilization; developmental stage (gestation period): between pectoral fin and jaw formation stage[18]) surface fish was used for SFL and 3 dpf Pachón fish for CFL. Embryo extract was made as follows: 3 dpf embryos were collected (minimum 200 embryos) and rinsed with Ringer's solution. The embryos were then homogenized in Leibovitz's L-15 media supplemented with 2 × Penicillin–Streptomycin (PS) (Thermo Fisher #10378016) (1 ml media per 200 embryos) using the tight pestle of a Dounce homogenizer. The extract was centrifuged to remove the debris and the supernatant collected and frozen in 1 ml aliquots at − 20 °C.

Liver tissue preparation and primary cell derivation. The cell line derivation was done from livers of ~ 150 days old fish. While the surface fish were not pre-conditioned before dissection, we starved Pachón fish for 1 week prior to liver dissection. As cavefish livers store more fat than the surface fish livers, we believe the starvation reduced the fat content in the livers which helped in the overall survival of the cells in vitro. The fish were euthanized in MS-222 and livers were dissected. The tissues, each weighing around 20 mg, were then quickly rinsed once in 70% alcohol, and washed multiple times with phosphate buffered saline (PBS) supplemented with 500 µg/ml of Penicillin–Streptomycin cocktail (final concentration of 5 ×). Each well of a 6-well plate contained 1–2 livers. The tissue was minced with a scalpel and trypsinized at room temperature (RT) for 5 min. Tissue was further disintegrated by pipetting up and down about 20 times with a 1 ml pipette tip during the incubation. The dissociated cells were then transferred to 15 ml conical tubes. Cells from one well were split to 2 × 15 ml tubes and pelleted at RT at 1000 rpm for 4 min. The cells were resuspended in 1 ml of ZFL-c + 1 × PS + 5% embryonic extract. 1 ml of cell suspension was seeded in one well of 48-well plate (gelled with 0.1% Gelatin at RT for 0.5 h) (Note: Cells from one liver (~ 20 mg) can be seeded to 2 wells of 48-well plate, approximately).

Cell line establishment. We replaced half of the culture media in each well with fresh media after 24 h. The media was changed every 2 days (we replaced only half of the old media to provide 50% conditioned media to the cells). Cells were passaged in a 1:2 ratio every week. Once the cells reached the T-25 flask, $1–2 \times 10^6$ cells were frozen for back up (Note: massive cell death is observed initially but a significant number of cells will attach and eventually grow). To obtain homogeneous cell populations, cell cloning by serial dilution method was performed according to the standard protocol from Corning (https://www.corning.com/catalog/cls/documents/protocols/Single_cell_cloning_protocol.pdf). In brief, the heterogeneous cells were serially diluted in 96-well plates and single cell colonies were picked once they became large and conspicuous. The SFLs were at passage #37 and the CFLs at #33 when the serial dilutions were performed. Once the clones reached 6-well plates, clones that had similar and homogeneous morphology between SFL and CFL were chosen for further characterization.

Preparation of metaphase spreads and chromosome counting. The cells were seeded in T-25 flasks to a density of 1×10^6 the day before chromosome preparation. On the next morning, 0.25% final concentration of colchicine was added to the cells and incubated for 2 h. The cells were collected and washed in PBS, centrifuged at 300×*g* for 3 min at RT. Hypotonic solution (0.075 M KCl) was applied to the cell pellet, incubated for 15 min at RT, and centrifuged at 188×*g* for 3 min at RT. Freshly prepared ice-cold fixative (75% Methanol, 25% glacial acetic acid) was added to the cell pellet, and the tube was kept on ice for 10 min. The suspension was centrifuged at 188×*g* for 5 min at 4 °C, and the pellet was resuspended in cold fixative. After 10 min incubation on ice, the suspension was centrifuged, resuspended in cold fixative one more time, and stored at − 20 °C until use. For the preparation of metaphase spreads, the cell suspension was dropped on a slide, and the slide was dried on a heat block at 75 °C for 3 min. Slides were stained with DAPI (10 µg/ml) for 10 min, and Prolong gold was applied as a mounting media. For chromosome counting, at least 88 metaphase spreads were analyzed using Zeiss Axio Vert 200M fluorescence microscope (Carl Zeiss, Jena, Germany) equipped with a 63 × N.A. 1.4 oil-immersion objective (Carl Zeiss, Jena, Germany). Image analysis and processing were performed using ImageJ software.

Genotyping. A PCR-based assay was used to determine the sex of the CFL cells according to published protocol[19]. Primer P5 and P6 were used. P5: TTTCTGACTGTTGGCCACCA. P6: CACCTCACAGAACGA CCTCC. Genomic DNA from tissues of male and female Pachón fish were taken as controls.

Seahorse assay. We followed the procedure described in the Seahorse Glycolysis Stress Test kit. In brief, 30,000 cells were seeded in each well of a 96-well plate one day prior to the day of experiment. Each cell line had 40 replicates on the same plate. On the day of experiment, the plate was placed in the BioTek Cytation system for brightfield imaging to count cells for normalization of the results. The plate was next transferred to the microplate stage of a Seahorse XFe96 flux analyzer (Seahorse). The initial extracellular acidification rate (ECAR) measurements were taken in the absence of glucose using a 3-min mix and 3-min read cycling protocol. Three separate readings were taken to ensure stability. Next, glucose was added to each well to a concentration of 10 mM, and three separate ECAR readings were taken. This was followed by an injection of oligomycin and Hoechst 33342. The final concentration of oligomycin in each well was 2 µM, and three separate ECAR readings were taken. Next, 2-deoxyglucose was injected to a final concentration of 25 mM in each well, and three separate ECAR readings were taken. XFe data normalization was performed by in situ nuclear staining and in situ cell counting using the imaging and normalization system (BioTek Cytation). The observations were derived from an experiment comprising of 40 technical replicates for each cell line.

ALT assay. Cells were grown to 80% confluency and 1×10^6 cells were collected as pellets in duplicates for the assay. Colorimetric assay to measure alanine aminotransferase activity in the cell lines was performed using the ALT activity assay kit from Sigma (MAK052-1KT) according to the manufacturer's instructions. Zebrafish Liver cell line was used as positive control.

Antibiotic kill curve. We plated cells at 90% per well of a 12-well plate. We kept 1 well in maintenance media as control. We set the remaining wells in chosen selection concentrations and ensured that the cells are from a healthy, routinely sub-cultured stock. We observed the culture daily and changed media with corresponding antibiotic concentrations. We determined which concentration to use by observation and chose the concentration 100 µg/ml of G418 above the concentration that has 100% cell death.

RNA-seq. RNA was extracted from adult liver and muscle tissues using Qiagen RNeasy kit according to manufacturer's instructions. Libraries were generated from 250 ng of high-quality total RNA, as assessed using the Bioanalyzer (Agilent). Libraries were made according to the manufacturer's directions using the TruSeq Stranded mRNA Library Prep kit (48 Samples) (Illumina, Cat. No. 20020594), and TruSeq RNA Single Indexes Sets A and B (Illumina Cat. No. 20020492 and 20020493). Resulting short fragment libraries were checked for quality and quantity using the Bioanalyzer (Agilent) and Qubit Fluorometer (Life Technologies). Libraries were pooled, quantified, and sequenced as 75 bp single reads on a high-output flow cell using the Illumina NextSeq 500 instrument. Following sequencing, Illumina Primary Analysis version RTA 2.4.11 and bcl2fastq2 v2.20 were run to demultiplex reads for all libraries and generate FASTQ files.

Alignment and differential expression: RNA-seq reads were aligned to *Astyanax mexicanus* reference genome from University of California at Santa Cruz using STAR version 2.7.3 with gene model retrieved from Ensembl, release 102 to generate gene read counts. The transcript abundance 'TPM' (Transcript per Million) was quantified using RSEM version 1.3. Differentially expressed genes were determined using R package edgeR version 3.30.3 after filtering low expressed genes with a CPM (Counts Per Million) of 0.2 in at least one library. The resulting p-values were adjusted with Benjamini–Hochberg method using R function p.adjust. Genes with an adjusted p-value < 0.05 and a fold change of 2 were termed as differentially expressed.

Functional enrichment or gene ontology (GO) analysis: Gene functional enrichment analysis was performed on the differentially expressed genes identified in edgeR. A custom wrapper around R package 'clusterProfiler' with gene-GO terms retrieved from Ensembl BioMart was used to identify over-represented GO terms in the differentially expressed genes compared with the background list of all genes.

Heatmap. To construct the liver cell line marker genes, we performed differential expression analysis between liver tissue and skeletal muscle samples using edgeR. Low expressed genes with CPM < 10 in at least one library were filtered prior to differential testing. The resulting p-values were adjusted with Benjamini–Hochberg method using R function p.adjust. Genes with an adjusted p-value < 0.01 and a fold change of 20 were termed as differentially expressed. The upregulated genes in liver tissue were compared to liver cell line data and the top 100 most expressed genes in liver cell line were selected. Heatmap of genes expressed in both liver tissue and liver cell lines but not in muscle was generated using R package pheatmap.

Statistical analysis. For all the results plotted as graphs (Figs. 1, 3, 4), we performed statistical analysis using Student's *t* test. Statistical analysis for RNA-seq data was performed using the R package edgeR.

Results

We derived cell lines from surface fish and Pachón cavefish livers using dissected livers from 5-month-old fish. The initial set of derived cell population was very heterogeneous, and we performed serial dilutions to isolate clonal cell populations. From the primary derivation, the cell lines have now been in culture for > 60 passages. The clonal populations were derived at passage #37 for SFL and #33 for CFL. The cells have an epithelial cell-like morphology and adhere to the culture plate surface (Fig. 1a,b). They are easy to maintain in a media containing

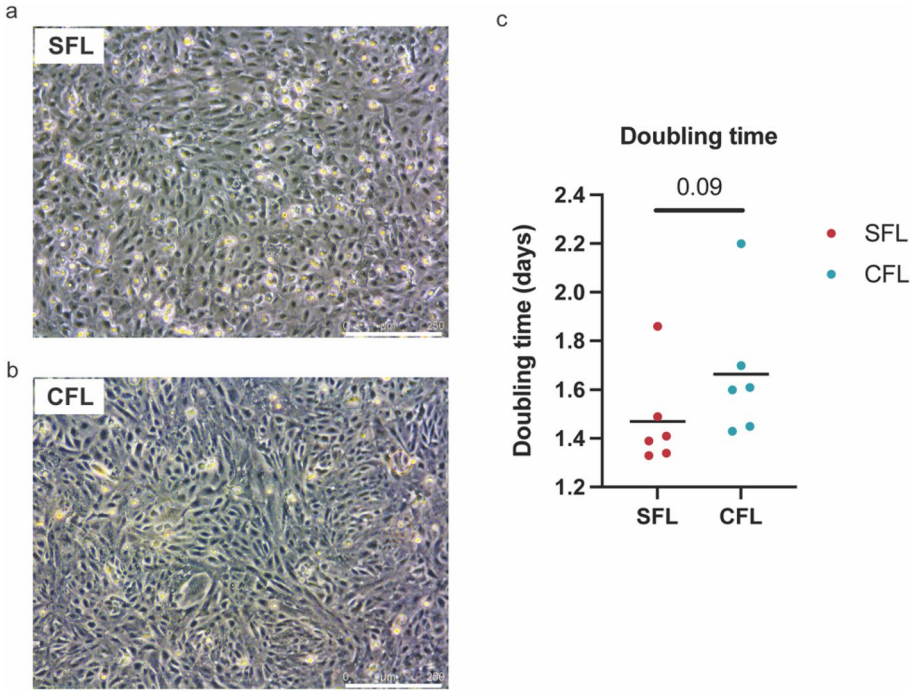

Figure 1. Brightfield images of SFL (**a**) and CFL (**b**). The scale denotes 250 µM. (**c**) Graph showing the calculated doubling time for the two cell lines. p-value was calculated using two-tailed Student's *t* test.

DMEM, L-15, Ham's F-12, trout, and fetal bovine serums, supplemented with insulin and epidermal growth factor and are passaged every week. Initial passages required supplementing the media with 5% *Astyanax* embryo extract (see "Methods" for details), however, once cultures became stable (passage 17 for SFL and passage 12 for CFL) the embryo extract was removed without affecting cell survival. All other components were found to be indispensable for cell survival. For routine passaging, the cells were trypsinized with TrypLE express (Thermo Fischer) for 3–4 min and pelleted by centrifugation at 130*g*, washed with PBS and seeded in desired density. We observed the growth curve for the two cell lines and calculated their doubling times using standard formula (Roth V. 2006 Doubling Time Computing, Available from: http://www.doubling-time.com/compute.php). Both the cell lines had a comparable doubling time with SFL dividing ~ 13% faster than CFL on average.

Karyotyping. Metaphase chromosome spreads were made for karyotyping the cell lines (Fig. 2a,b). We observed a modal chromosome number of 50 (haploid chromosome number n = 25) for the SFL which was equal to the physiological chromosome count as revealed by genome sequencing[20]. The CFL cell line was hyperdiploid with a modal chromosome count of 58 (haploid chromosome number n = 29) (Fig. 2c). A recent study showed that Pachón males have B chromosomes[19] and we suspected that some of these extra chromosomes could be B chromosomes. B chromosomes are supernumerary and non-essential chromosomes with non-Mendelian inheritance found in many plant and animal species. They are mainly non-coding and heterochromatic, but some contain coding genes as well. In *Astyanax mexicanus*, B chromosomes containing the *gdf6b* gene have been found to be strongly male predominant[19]. As the fish used to derive the cell lines were sub-adults, we were unable to determine the sex of those fish at time of dissection. To test if the CFL are of male origin and contain B chromosomes, we performed a PCR based assay as described in[19] (Fig. 2d). We detected the presence of B chromosomes in the CFL suggesting that the fish used to derive the CFL was indeed a male (Fig. 2d, Supplementary Fig. 3). We were unable to test the sex of the SFL due to the lack of a similar assay for surface fish.

SFL and CFL express liver-specific enzymes. Liver tissue is characterized by the production of liver-specific enzymes such as alanine aminotransferase (ALT) and aspartate aminotransferase. To test for liver-specific activity levels in these cell lines, we performed ALT assay and used a zebrafish liver cell line (ZFL) as control (see Supplementary Fig. 1 for standard curves). We observed ALT activity in both the cell lines (Table 1).

CFL have increased glycolysis. Previous studies have shown drastic metabolic differences in the metabolism of surface fish and cavefish[4,5,21]. Most of the differences that have been documented affect glucose and fat metabolism pathways. For example, it has been shown that surface fish have increased fat catabolism while cavefish have increased fat anabolism[4,21]. Furthermore, metabolomic analysis of liver tissues show that cavefish have increased glycolysis as compared to surface fish[5]. To test if the energy metabolism of the corresponding cell lines shows similar differences between the morphotypes, we performed two rounds of glycolytic stress test using the Seahorse Analyzer according to the manufacturer's instruction and published protocols[22] (Fig. 3). The analyzer measures the Extracellular Acidification Rate (ECAR) which is the rate of decrease in pH in the assay media

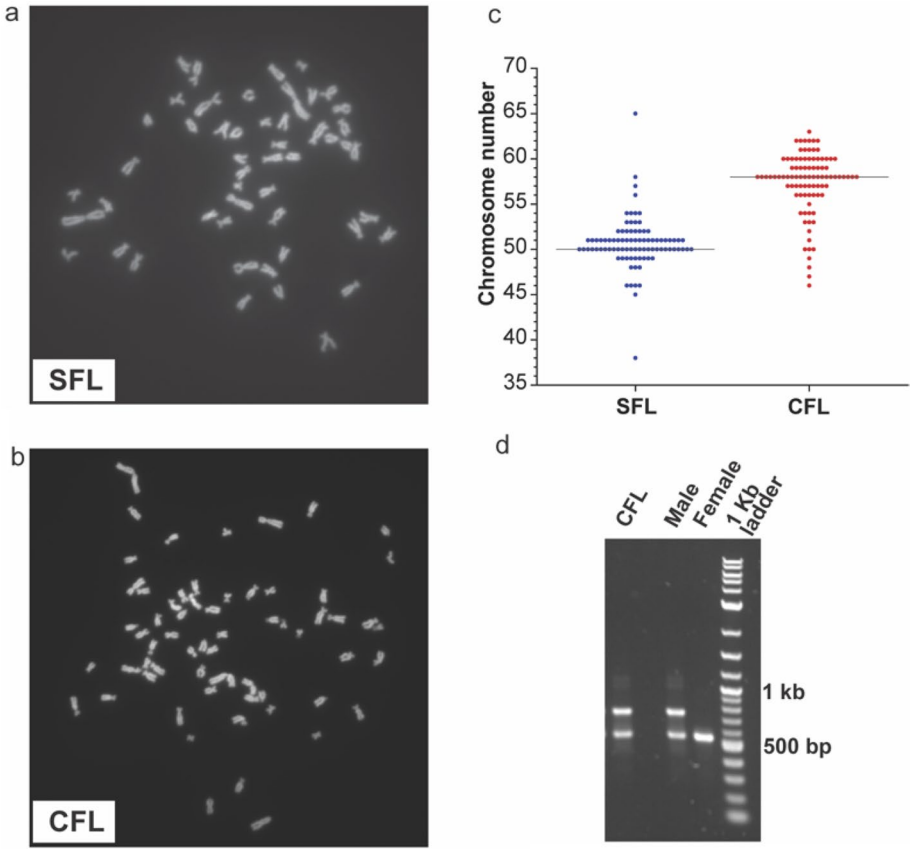

Figure 2. (**a**) Representative chromosome spread for SFL. (**b**) Representative chromosome spread for CFL. (**c**) The graph shows the chromosome counting for 88 and 92 spreads respectively for SFL and CFL. (**d**) Gel picture showing products obtained from PCR on genomic DNA using primers to determine sex in Pachón cavefish. Presence of the higher molecular weight band indicates the presence of a B chromosome, and the sex is determined as male.

Cell line	Activity (milliunits/ml)
SFL	3.940
CFL	1.577
ZFL	0.882

Table 1. The table shows the ALT activity levels of the cell lines.

and provides the rate of glycolysis. It also provides the Oxygen Consumption Rate (OCR), which is the rate of decrease of oxygen concentration in the assay media and gives a measure of the rate of mitochondrial respiration of the cells. To better understand glycolysis, we focused on the ECAR data per the manufacturer's instructions (Fig. 3a). We observed an increased basal level of glycolysis in CFL at the beginning of the experiment. The difference continued even after the addition of glucose, indicating the ability of CFL to perform increased glycolysis (Fig. 3a). Upon addition of oligomycin, a chemical that inhibits aerobic respiration causing the cells to rely on glycolysis for energy, the cavefish cells showed a higher acidification rate indicating their ability for increased glycolysis (Fig. 3a). The OCR measurements revealed a slightly lower mitochondrial respiration for CFL than for SFL (Fig. 3b). Thus, in combination (Fig. 3c) this data shows higher glycolysis in CFL with a slightly lower level of oxygen consumption. In effect, the CFL rely more on oxygen independent methods of energy production as compared to the SFL which is in line with our previous observations using liver tissue metabolomics[5]. The results underscore the utility of these cell lines for future metabolic characterization in an in vitro system.

Transcriptome analysis shows increased lipid catabolism in SFL. Next, to characterize the gene expression in the cell lines, we analyzed their transcriptomes using bulk-RNA-seq. All the samples yielded quality reads with the 3 replicates highly correlated and clustered together (Supplementary Fig. 2a). We observed expression of ALT (*gpt*, *gpt2l*) genes (Supplementary Fig. 2b) that supported the enzyme colorimetric assays

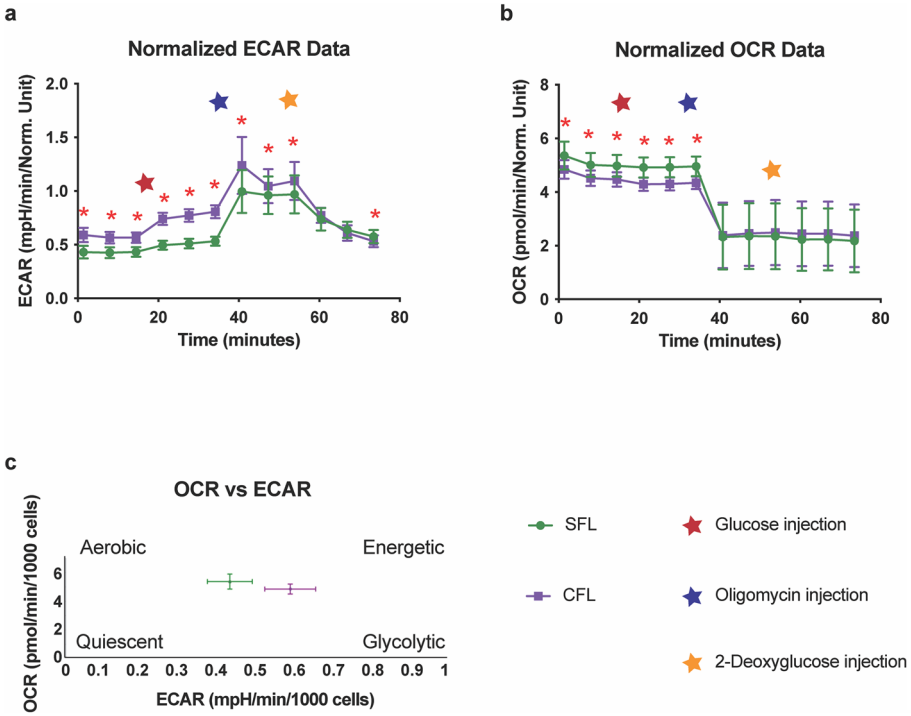

Figure 3. The figure shows results from the Seahorse assay. (**a**) Extracellular acidification rate (ECAR) for SFL and CFL. (**b**) Oxygen consumption rate (OCR) for SFL and CFL. (**c**) OCR vs ECAR graph reflecting increased glycolysis for CFL. * indicates p-value < 0.001 as calculated using a two-tailed Student's *t* test.

(Table 1), as well as several other important liver metabolism genes in both cell lines. These genes include lipid metabolism genes such as apolipoproteins, *stearoyl-coA desaturase* (*scdb*) and fatty acid desaturase (*fads2*) and master regulator genes such as *peroxisome proliferator-activated receptor* (*ppary*) and *peroxisome proliferator-activated receptor gamma coactivator 1a* (*pgc1a* or *ppargc1a*) (Fig. 4a). The expression of these genes is essential for lipid metabolism; *scdb* and *fads2* break down fat indicating active lipid metabolism in the cell lines[23]. Interestingly, the fat catabolizing gene *fads2* was upregulated in SFL. This is in line with the observed physiology of the fish wherein surface fish have less fat and undergo more catabolic processes while cavefish are obese with increased anabolic processes[4,10,21]. To broadly study the categories of genes that are differentially regulated between the two cell lines, we performed differential gene expression analysis. We observed 2472 downregulated genes and 2791 upregulated genes in SFL as compared to CFL. While genes upregulated in CFL were not enriched for any metabolism GO term, the genes upregulated in SFL were enriched for GO terms 'lipid metabolic process', 'lipid catabolic process' and several immune system related GO terms such as 'complement activation' and 'activation of immune response' (Fig. 4b,c). For instance, genes under the 'lipid catabolic process' such as *lipase ɛb* (*lipeb*), *carnitine palmitoyltransferase 1a* (*cpt1aa*), *phospholipase D1* (*pld1b*) and genes comprising GO terms related to immune system such as *complement component c3b* (*c3b.2*), *G protein-coupled receptor 1* (*gpr1*), and *thymocyte expressed, positive selection associated 1* (*tespa1*) are all upregulated in SFL as compared to CFL (Fig. 4d,e). *cpt1aa* is involved in fatty acid oxidation, *lipeb* breaks down triglycerides and *pld1* feeds into the mTOR pathway to regulate fat levels[24–26]. Further, *c3b* is involved in apoptosis and phagocytosis, *gpr1* influences glucose levels and *tespa1* is required for B-cell activation[27–29]. These results reflect the biology of these fishes in vivo, as it has been shown that surface fish undergo higher lipid breakdown while cavefish synthesize more lipid and surface fish have an increased innate immune response compared to cavefish[5,7,21].

Surprisingly, we also observed enrichment of GO terms seemingly unrelated to liver physiology among genes upregulated in CFL. These were related to the nervous system and eye development. We were curious to know why such GO terms would be enriched in a liver-derived cell line. A closer examination of the genes comprising these GO terms revealed pleiotropic genes that were involved not just in eye or nervous system development, but rather genes expressed in multiple tissues involved in many other processes as well. We observed that many of these genes such as *sox11b* (under 'closure of optic fissure') are transcription factors high up in the hierarchy involved in many physiological processes. Another example is *arl6*, a gene that causes Bardet-Biedl Syndrome 3 that leads to defects not only in sensory and visual perception but is also related to obesity (https://omim.org/entry/600151#description). Hence, we believe, that some of the GO term enrichments could partly be the result of incomplete annotation of *Astyanax* gene function. Hence, we focused only on GO terms that we can infer the relevance in this tissue/cell type (Fig. 4a,d,e), however, it is tempting to speculate that some of the pleiotropic genes that we found to be differentially expressed in the liver may be involved in the eye loss phenotypes characteristic of cavefish[30].

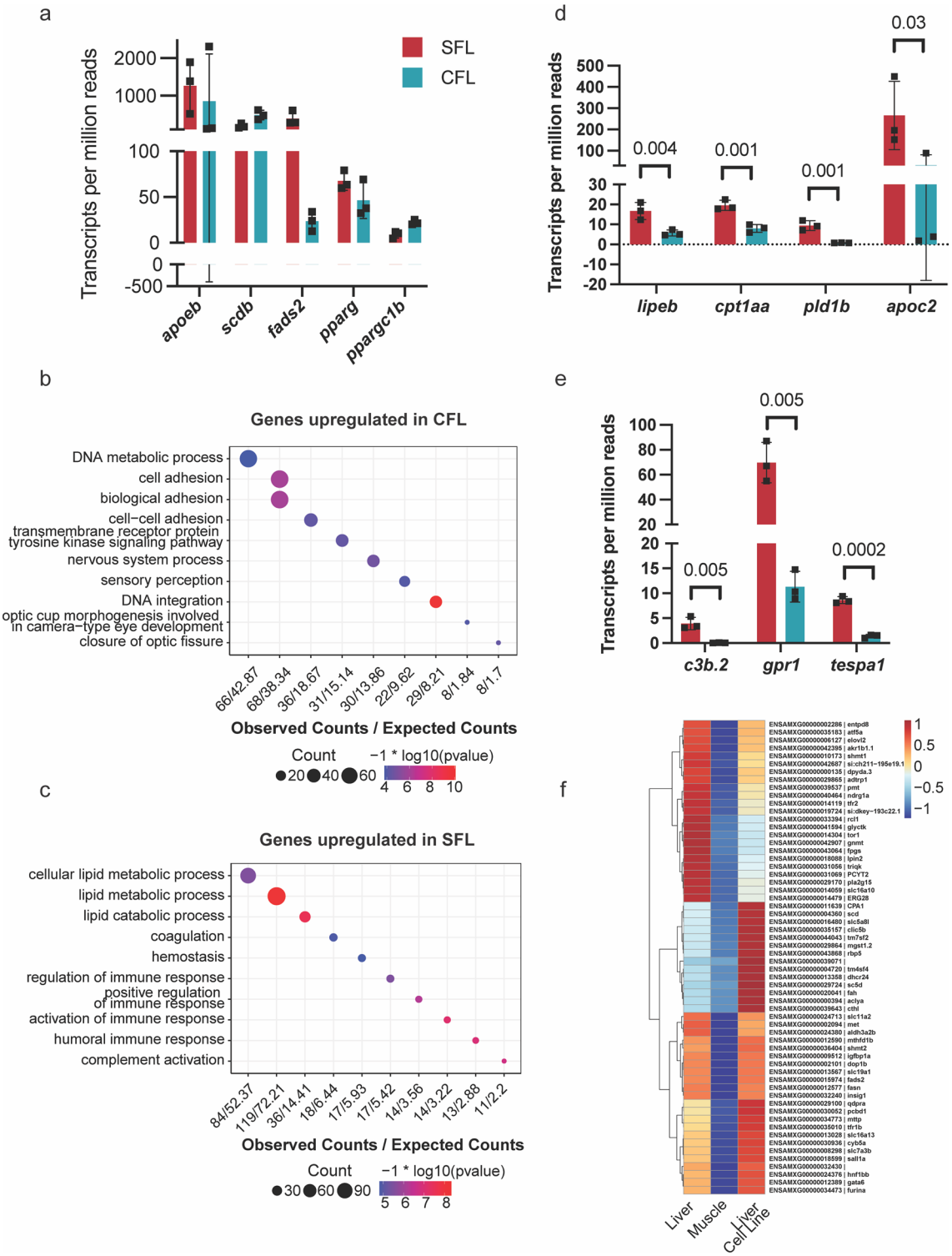

Figure 4. (**a**) Expression levels for key liver metabolism genes. (**b**) GO terms enriched among genes upregulated in SFL vs CFL. (**c**) GO terms enriched among genes downregulated in SFL vs CFL. (**d**) Genes belonging to 'lipid catabolic process' that are upregulated in SFL. (**e**) Genes belonging to 'activation of immune response' that are upregulated in SFL. The bar graphs represent standard deviation around mean values. (**f**) Heatmap depicting average gene expression levels of genes that are not expressed in the muscle but are expressed in both liver tissue and liver cell lines. p-values were calculated using a two-tailed Student's *t* test.

Next, we intended to compare the cell line gene expression to gene expression in vivo. To that end we first generated a set of liver specific marker genes, by generating bulk RNA-seq data for skeletal muscle tissue and

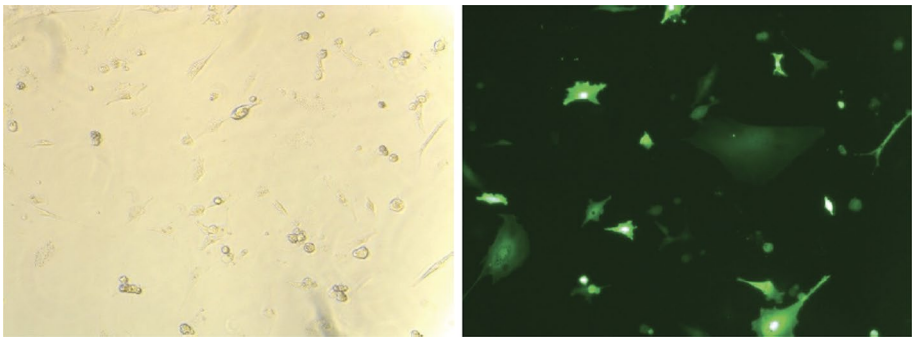

Figure 5. Brightfield and fluorescence images of SFL electroporated with pMaxGFP plasmid.

compare expression to previously published bulk transcriptome data from liver tissue[4]. This set of genes was then compared to the cell line transcriptome data to annotate a gene list that expresses in the liver tissue and cell lines but not in the muscle (Fig. 4f, Supplementary Table 1). Many of these genes belong to liver metabolism pathways such as *scd, fatty acid synthase* (*fasn*), *fads2, lipin 2* (*lpin2*) *and hepatocyte nuclear factor 1bb* (*hnf1bb*). *lpin2* is involved in triglyceride metabolism; *hnf1b* is essential for liver development and mutations in it cause diabetes in humans[31]. This gene set is a useful resource for many downstream studies using these cell lines and provides a proof of active metabolic pathways in these cell lines (Supplementary Table 1).

SFL and CFL can be used for generating transgenics. Through the availability of robust gene editing techniques, it has become possible to easily generate gene knockouts in cell lines. Furthermore, cell lines provide an efficient platform for protein overexpression for the study of cell biology and to perform biochemical assays. Thus, to maximize the utility of these cell lines, we tested their ability to be transfected/electroporated. We transfected CFL with a plasmid that expresses GFP under the CMV promoter. We attained good success with transgene expression using electroporation with Lonza nucleofection in CFL (Fig. 5). Furthermore, to aid in generation of stable cell lines, we performed kill curves to determine the minimum concentration of G418 needed to kill untransfected cells without affecting the transfected cells. Concentrations ranging from 0 to 1200 µg/ml were tested. We observed complete cell death with 600 µg/ml concentration. These experiments show that the cell lines can be transfected using standard transfection protocols and will increase the utility of these cell lines to study liver metabolism in cavefish.

Conclusions

In this study, we have generated the first in depth characterized cell lines from *Astyanax mexicanus*. These liver derived cell lines are adherent and have epithelial/endodermal-like morphology and are easily maintained and sub-cultured in standard tissue culture conditions. The cells express liver enzyme alanine aminotransferase as well as many other key liver metabolism genes. The energy metabolism parameters mirror the in vivo liver physiology of these fish. We also show that these cells are amenable to electroporation that further enhances their utility as in vitro models. The cell lines thus serve as excellent in vitro systems to study and elucidate metabolic features governing the adaptation of cavefish to nutrient poor cave habitats.

Data availability

Original data underlying this manuscript can be accessed from the Stowers Original Data Repository at http://www.stowers.org/research/publications/libpb-1676. The RNA-seq data can be found at GEO accession number GSE195950.

Received: 27 January 2022; Accepted: 8 June 2022
Published online: 16 June 2022

References

1. Scherer, W. F., Syverton, J. T. & Gey, G. O. Studies on the propagation in vitro of poliomyelitis viruses. IV. Viral multiplication in a stable strain of human malignant epithelial cells (strain HeLa) derived from an epidermoid carcinoma of the cervix. *J. Exp. Med.* **97**, 695–710 (1953).
2. Aspiras, A. C., Rohner, N., Martineau, B., Borowsky, R. L. & Tabin, C. J. Melanocortin 4 receptor mutations contribute to the adaptation of cavefish to nutrient-poor conditions. *Proc. Natl. Acad. Sci. U.S.A.* **112**, 9668–9673 (2015).
3. Krishnan, J. *et al.* Comparative transcriptome analysis of wild and lab populations of *Astyanax mexicanus* uncovers differential effects of environment and morphotype on gene expression. *J. Exp. Zool. B Mol. Dev. Evol.* **334**, 530–539 (2020).
4. Krishnan, J., Seidel, C.W., Zhang, N., VanCampen, J., Peuß, R., Xiong, S., Kenzior, A., Li, H., Conaway, J. W. & Rohner, N. Genome-wide analysis of *cis*-regulatory changes in the metabolic adaptation of cavefish. *bioRxiv* (2020).
5. Medley, J. K., Persons, J., Biswas, T., Olsen, L., Peuß, R., Krishnan, J., Xiong, S. & Rohner, N. Resilience in a natural model of metabolic dysfunction through changes in longevity and ageing-related metabolites. *bioRxiv* (2021).
6. Olsen, L., Thum, E. & Rohner, N. Lipid metabolism in adaptation to extreme nutritional challenges. *Dev. Cell* **56**, 1417–1429 (2021).
7. Peuss, R. *et al.* Adaptation to low parasite abundance affects immune investment and immunopathological responses of cavefish. *Nat. Ecol. Evol.* **4**, 1416–1430 (2020).
8. Riddle, M. R. *et al.* Insulin resistance in cavefish as an adaptation to a nutrient-limited environment. *Nature* **555**, 647–651 (2018).

9. Rohner, N. Sweet fish: Fish models for the study of hyperglycemia and diabetes. *J. Diabetes* **11**, 193–203 (2019).
10. Xiong, S., Krishnan, J., Peuss, R. & Rohner, N. Early adipogenesis contributes to excess fat accumulation in cave populations of *Astyanax mexicanus*. *Dev. Biol.* **441**, 297–304 (2018).
11. Cavallari, N. *et al.* A blind circadian clock in cavefish reveals that opsins mediate peripheral clock photoreception. *PLoS Biol.* **9**, e1001142 (2011).
12. Pagano, C. *et al.* Evolution shapes the responsiveness of the D-box enhancer element to light and reactive oxygen species in vertebrates. *Sci. Rep.* **8**, 13180 (2018).
13. Mirabelli, P., Coppola, L. & Salvatore, M. Cancer cell lines are useful model systems for medical research. *Cancers (Basel)* **11**, 1098 (2019).
14. Nikolic, M., Sustersic, T. & Filipovic, N. In vitro models and on-chip systems: Biomaterial interaction studies with tissues generated using lung epithelial and liver metabolic cell lines. *Front. Bioeng. Biotechnol.* **6**, 120 (2018).
15. Thangaraj, R. S. *et al.* Comprehensive update on inventory of finfish cell lines developed during the last decade (2010–2020). *Rev. Aquac.* **13**, 2248–2288 (2021).
16. Kilkenny, C., Browne, W. J., Cuthill, I. C., Emerson, M. & Altman, D. G. Improving bioscience research reporting: The ARRIVE guidelines for reporting animal research. *PLoS Biol.* **8**, e1000412 (2010).
17. Ghosh, C., Zhou, Y. L. & Collodi, P. Derivation and characterization of a zebrafish liver cell line. *Cell Biol. Toxicol.* **10**, 167–176 (1994).
18. Hinaux, H. *et al.* A developmental staging table for *Astyanax mexicanus* surface fish and Pachon cavefish. *Zebrafish* **8**, 155–165 (2011).
19. Imarazene, B. *et al.* A supernumerary "B-sex" chromosome drives male sex determination in the Pachon cavefish, *Astyanax mexicanus*. *Curr. Biol.* **31**, 4800-4809 e4809 (2021).
20. Warren, W. C. *et al.* A chromosome-level genome of *Astyanax mexicanus* surface fish for comparing population-specific genetic differences contributing to trait evolution. *Nat. Commun.* **12**, 1447 (2021).
21. Xiong, S., Wang, W., Kenzior, A., Olsen, L., Krishnan, J., Persons, J., Medley, K., Peuss, R., Wang, Y., Chen, S. *et al.* Enhanced lipogenesis through Ppargamma helps cavefish adapt to food scarcity. *Curr. Biol.* (2022).
22. Wilkins, H. M. *et al.* Oxaloacetate enhances neuronal cell bioenergetic fluxes and infrastructure. *J. Neurochem.* **137**, 76–87 (2016).
23. Bechmann, L. P. *et al.* The interaction of hepatic lipid and glucose metabolism in liver diseases. *J. Hepatol.* **56**, 952–964 (2012).
24. Song, H. I. & Yoon, M. S. PLD1 regulates adipogenic differentiation through mTOR-IRS-1 phosphorylation at serine 636/639. *Sci. Rep.* **6**, 36968 (2016).
25. Schlaepfer, I. R. & Joshi, M. CPT1A-mediated fat oxidation, mechanisms, and therapeutic potential. *Endocrinology* **161**, bqz046 (2020).
26. Reid, B. N. *et al.* Hepatic overexpression of hormone-sensitive lipase and adipose triglyceride lipase promotes fatty acid oxidation, stimulates direct release of free fatty acids, and ameliorates steatosis. *J. Biol. Chem.* **283**, 13087–13099 (2008).
27. Rourke, J. L., Muruganandan, S., Dranse, H. J., McMullen, N. M. & Sinal, C. J. Gpr1 is an active chemerin receptor influencing glucose homeostasis in obese mice. *J. Endocrinol.* **222**, 201–215 (2014).
28. Xu, W. *et al.* Properdin binds to late apoptotic and necrotic cells independently of C3b and regulates alternative pathway complement activation. *J. Immunol.* **180**, 7613–7621 (2008).
29. Yao, Y. *et al.* Tespa1 deficiency dampens thymus-dependent B-cell activation and attenuates collagen-induced arthritis in mice. *Front. Immunol.* **9**, 965 (2018).
30. Krishnan, J. & Rohner, N. Cavefish and the basis for eye loss. *Philos. Trans. R. Soc. Lond. B Biol. Sci.* **372**, 20150487 (2017).
31. El-Khairi, R. & Vallier, L. The role of hepatocyte nuclear factor 1beta in disease and development. *Diabetes Obes. Metab.* **18**(Suppl 1), 23–32 (2016).

Acknowledgements

The authors would like to thank the cavefish team for animal husbandry, and Xiaowan Wang and Heather Wilkins from University of Kansas Medical Center for the support on Seahorse assay. This work is supported by institutional funding, NIH Grant 1DP2OD028806-01 and EDGE award 1923372.

Author contributions

J.K. and N.R.O. conceived the project, J.K., Y.W. (Yan), O.K., and C.Z. generated the cell line. J.K., O.K., L.O., D.T. and A.K. characterized the cell line with support from Y.W. (Yongfu). J.K., R.P. and S.X. generated the muscle RNA-seq data. H.H. and J.K. analyzed the transcriptome data. J.K. and N.R. wrote the manuscript and all authors read and approved it.

Competing interests

The authors declare no competing interests.

Additional information

Supplementary Information The online version contains supplementary material available at https://doi.org/10.1038/s41598-022-14507-0.

Correspondence and requests for materials should be addressed to J.K. or N.R.